



# HHS Public Access

Author manuscript

*IEEE/ACM Trans Comput Biol Bioinform.* Author manuscript; available in PMC 2020 May 01.

Published in final edited form as:

*IEEE/ACM Trans Comput Biol Bioinform.* 2019 ; 16(3): 1007–1019. doi:10.1109/TCBB.2017.2756930.

## Parallel stochastic discrete event simulation of calcium dynamics in neuron

**Mohammad Nazrul Ishlam Patoary,**

School of Computer Science, McGill University, Canada

**Carl Tropper,**

School of Computer Science, McGill University, Canada

**Robert A. McDougal,**

Yale University, USA

**Zhongwei Lin,** and

National University of Defense Technology Changsha, Hunan, China

**William W. Lytton**

SUNY Downstate Medical Center, USA

### Abstract

The intra-cellular calcium signaling pathways of a neuron depends on both biochemical reactions and diffusions. Some quasi-isolated compartments (e.g. spines) are so small and calcium concentrations are so low that one extra molecule diffusing in by chance can make a nontrivial difference in concentration (percentage-wise). These rare events can affect dynamics discretely in such way that they cannot be evaluated by a deterministic and continuous simulation. Stochastic models of such a system provide a more detailed understanding of these systems than existing deterministic models because they capture their behavior at a molecular level. Our research focuses on the development of a high performance parallel discrete event simulation environment, Neuron Time Warp (NTW), which is intended for use in the parallel simulation of stochastic reaction-diffusion systems such as intra-calcium signaling. NTW is integrated with NEURON, a simulator which is widely used within the neuroscience community. We simulate two models, a calcium buffer and a calcium wave model. The calcium buffer model is employed in order to verify the correctness and performance of NTW by comparing it to a sequential deterministic simulation in NEURON. We also derived a discrete event calcium wave model from a deterministic model using the stochastic IP<sub>3</sub>R structure.

### Index Terms

PDES; NSM; NTW; discrete event calcium wave model; parallel stochastic discrete event simulation

## 1 Introduction

The human brain may be viewed as a densely connected network of approximately 86 Billion neurons [1]. As is well known, the neuron is the computational building block of the

human brain. Each neuron receives inputs from thousands of other neurons via its dendrites and in turn connects to thousands of other neurons via its axon. The point of contact between the axon and the dendrite of another neuron is called the synapse. The inter-cellular space between the presynaptic and postsynaptic neurons is called the synaptic space or synaptic cleft. When a synapse is activated by an electrical impulse from a presynaptic neuron, it releases chemical substances (called neurotransmitters) into the synaptic cleft which diffuse across the synaptic space to the post-synaptic neuron. The neurotransmitter molecules can then bind to special receptors located on the membrane of the postsynaptic neuron. Receptors are membrane proteins that are able to bind a specific chemical substance, such as a neurotransmitter.

The membrane of a neuron is semi-permeable and has ion channels within it which control ion flow (including sodium, potassium, and calcium) between the exterior and the interior of the cell body. Movements of ions through these channels result from the diffusion of the ions down concentration gradients and the voltage difference created by different concentrations of these ions on the exterior and the interior of the membrane. Some of the channels are voltage gated; they are controlled, i.e. opened or closed, by the electrical membrane potential.

Neurons use a number of signaling pathways to regulate their internal activity. A signaling pathway is initiated when an extracellular molecule activates a specific receptor located on the cell surface. In turn, this receptor triggers a biochemical chain of reactions and/or diffusions inside the cell and then creates a response. These signaling pathways fall into two main groups depending on how they are activated. Many of them are activated by external stimuli and the cell responds to both intra- and extra-cellular cues, and it can detect these through various signaling cascades wherein molecules react, diffuse, and/or are transported. Others respond to information generated from within the cell, usually in the form of metabolic messengers. In these signaling pathways information is conveyed either through protein-protein interactions or is transmitted via diffusing molecules which are referred to as second messengers. A second messenger is an intra-cellular substance, e.g. a calcium ion, that mediates cell activity by relaying a signal from an extracellular molecule, (e.g. a neurotransmitter) which is bound to the cell's surface. In this case the neurotransmitter is the first messenger. In a neuron, the calcium ion plays a crucial role in neuronal channel dynamics and ultimately in the behavior of the entire neuron [4]. It also acts as a second messenger in the cell and triggers processes such as initiating the biochemical cascades that lead to the changes in receptor insertion in the membrane. This underlies synaptic plasticity, the ability of synapses to strengthen or weaken over time in response to increases or decreases in their activity, to muscle contraction, and the secretion of neurotransmitters at nerve terminals. Because of the importance of calcium in neural transmission the accurate and efficient simulation of intra-cellular calcium dynamics has become an important research issue for neuroscientists.

Intra-cellular calcium signaling pathways make use of biochemical reactions as well as the diffusion of calcium ions. These pathways are an example of a reaction-diffusion system. Such a system describes the population dynamics of one or more species distributed in space which are propelled by two major events: reaction and diffusion. Partial differential equation

are commonly used to model such system and employ continuous simulation. These models are not very accurate, however, for a small number of ions in a small compartment such as a neuronal spine [4]. These compartments are so small and calcium concentrations are so low that several calcium molecules diffusing into them can make a nontrivial difference in their concentration. Again the concentrations in continuous simulators are expressed by real numbers instead of integers, resulting in incorrect behaviors. As a result stochastic discrete-event simulation has emerged as a method to complement differential equations in biochemical simulations [18] [14].

A system consisting of a collection of chemical reactions can be modeled by a chemical master equation. Such an equation models the distribution of the chemical reactants in the system [4] probabilistically for each point in time. In general, it is very difficult to solve this equation. In [5] Gillespie introduced a Monte Carlo simulation algorithm for this model. Under the assumption that the molecules of the system are uniformly distributed, the algorithm simulates a single trajectory of the chemical system. Simulating a number of these trajectories then gives a picture of the system. The algorithm uses an exponential distribution to compute the time of the next event (i.e. reaction) and employs elementary combinatorics to compute the likelihood of a particular reaction occurring.

[6] describes the Next Reaction Method, which attempts to reduce the computation time of the propensities in Gillespie's algorithm. It makes use of a dependency graph among the reactions which is used to identify the reactions which are in need of an update. Gillespie's algorithm then updates the states of all of the reactants. [8] modifies the Next Reaction Method by re-sorting the event queue in the order of the probability of execution of the reactions. A number of other efforts aimed at improving the efficiency of the Gillespie algorithm have been made, including [7], [9].

A key assumption in the Gillespie algorithm is that the particles are distributed homogeneously in space. This, however, is not the case because particles in neurons are not distributed homogeneously in space because neurons are so large that diffusion cannot equilibrate them and the diffusion of ions in a neuron takes place. This diffusive behavior must be included in a realistic model. Molecular dynamic simulations [10] [15] [16] could be used to model individual particles but take into account inter-particle forces, rendering them computationally expensive. Instead, we make use of a less expensive Monte Carlo algorithm, the Next Sub-volume Method (NSM) [11]. The NSM partitions space into cubes and represents the diffusion of ions between these cubes by events. Other events are used to characterize reactions within the cubes. NSM makes use of the Gillespie algorithm to compute next event times within the cubes and relies upon the use of a priority queue to determine the next event and diffusion times. Our parallel simulator, Neuron Time Warp (NTW), makes use of the NSM algorithm the reason that particles are not distributed homogeneously in neurons.

Calcium plays a pivotal role among the second messenger systems of a neuron. The mechanism by which calcium is transmitted in particular neuron domains is a subject of active research. Any model will surely not provide an accurate view of molecular dynamics within a cell. However, a stochastic reaction-diffusion simulator capable of working at scale

can help to provide a clearer understanding of calcium transmission. The sequential stochastic discrete event simulation of a large scale reaction-diffusion system is slow. Parallel Discrete Event Simulation (PDES) can be used to overcome this performance bottleneck [24]. Adapting PDES techniques to stochastic simulation using NSM was demonstrated in [22] [23] [24] [25]. In our research we employ real biological models which are of significance to neuroscientists.

This paper describes a parallel discrete event simulator, called NTW, which can be used to execute a 3D stochastic reaction-diffusion model. We use of NTW to simulate the calcium dynamics in a neuron. NTW is an optimistic simulator based on Time Warp. It makes use of a multi-level queue for the pending event set and a single rollback message in place of individual anti-messages. The multi-level queue structure disperses contention for the priority queue which naturally occurs in a parallel simulator. Single rollback messages decrease the overhead of Time Warp rollbacks.

We previously made use of a model of a dendrite branch on which to evaluate NTWs performance in [2]. We employed a spatial Lotka-Volterra model and verified the accuracy of the models. We evaluated the performance of NTW using MPI and shared memory models on a multi-core machine.

In this paper we make use of two models which simulate the calcium dynamics in a neuron- a calcium buffer and a calcium wave model. The calcium buffer model is employed to verify the correctness of NTW by comparing it to a sequential deterministic simulation in NEURON [3], a simulation environment in which complex nerve models can be created and simulated. It is widely used within the neuroscience community. We also examined NTW's performance using the calcium buffer model. We derived a discrete event calcium wave model from a deterministic model [33] [35] and used it to simulate a calcium wave in a neuron. We experimentally integrated NTW with NEURON.

The rest of the paper is structured as follows. Section 2 contains the background and related work while section 3 focuses on the experimental integration of NTW with NEURON. Section 4 describes NTW and section 5 contains experimental results. Section 6 is devoted to a description of future work and the conclusion.

## 2 Background and Related Work

There are two types of algorithms which have been used for stochastic simulation of neurons, particle-based and lattice-based [14]. In particle based methods, the state of the system is the number and location of particles in the sub-cellular space. The location of a particle and the system time are governed by probability distributions (e.g. the distribution in [14]). Particles engage in a reaction when they are close enough. MCell [15], Smoldyn [16] and CDS [17] are particle based simulators. In lattice-based methods, the sub-cellular space is subdivided into lattice points or voxels using a mesh generation algorithm, and molecules are represented within each voxel. NSM is a lattice-based algorithm, in which space is partitioned into mesh grids called sub-volumes (i.e. voxels). Reactions can happen between molecules in the same grid and molecules can diffuse to adjacent grids. As we employed the

next sub-volume method in which reactions between adjacent grids are ignored, we also ignored reactions between adjacent grids in NTW. STEPS [18] is a spatial extension of the Gillespie's Stochastic Simulation Algorithm (SSA), and NeuroRD [14] are based on a spatial extension of the Gillespie tau-leap algorithm. These tools develop sequential versions, while our intention is to produce a parallel algorithm capable of large scale simulations.

### 2.1 Next Sub-volume Method: NSM

NSM is a discrete-event approach to simulating both reactions and diffusion of species within a volume which contains an inhomogeneous distribution of particles [11]. The volume is divided into sub-volumes which are assumed to be well-stirred. Figure 1 contains such a computational sub-volume.

There are two types of events used in this approach: 1) those which represent reactions inside a sub-volume and 2) those which represent diffusion between adjacent sub-volumes. NSM makes use of the Gillespie algorithm to compute the next event time within a sub-volume. Within the main loop of the algorithm the sub-volume with the smallest next event time is selected and the event type is then determined using the reaction rates. The event is then executed and the state is updated. Note that the update is done only in a small region. NSM relies upon priority queues for both the next event time and the diffusion time.

### 2.2 Parallel Stochastic Discrete-Event Simulation

A PDES is composed of a set of processes which are executed on different processors. The processes model different parts of a physical system. Each process is referred to as a Logical Process (LP). The LPs communicate with each other via time stamped messages. Events are stored in an event list, Each LP processes its events in increasing time stamp order. The efficient management of the event list has a significant effect on the performance of the parallel simulation. Although processing the events in a sequential simulation is done by using a centralized list, such an approach is not possible in a parallel simulation as it would be too inefficient. Hence errors can result in a parallel simulation from out of order event execution (causality errors). The problem of maintaining causality is referred to as the synchronization problem - the idea is to make sure that the execution of the parallel simulation produces the same sequence of events as if all of the events had been processed by a single process. There are two main approaches for solving the synchronization problem-conservative and optimistic. Time Warp (TW) synchronization is a widely used optimistic synchronization protocol and is the one which we make use of in NTW [2].

NSM can be applied to PDES by discretizing space into sub-volumes and assigning a of sub-volumes to each LP. Interactions between LPs involve the diffusion of events between neighboring sub-volumes. In order to evaluate the parallel execution of the NSM algorithm, [22] uses two Time Warp based approaches. Both represent sub-volumes by LPs and messages between sub-volumes contain the diffusion events. One of the simulators makes use of grid computing. Preliminary results on small models were encouraging. As pointed out by the authors, a number of areas including window management and state saving remain to be investigated.

[23] points out that a conservative synchronization is not suitable for use with the NSM due to the zero lookahead property of the exponential distribution. An optimistic algorithm was implemented and preliminary results obtained for a predator-prey model (Lotka-Volterra). The performance of the simulation was hampered by a lack of control over the window size.

[24], [25] investigates the performance of optimistic synchronization algorithms in simulations of a reaction-diffusion system based on Gillespie's SSA [5]. They present a variant of the Next Sub-volume Method called the Abstract Next Sub-volume Method (ANSM). Three optimistic synchronization algorithms were employed: Time Warp (TW) [26], an optimistic approach with risk-free message sending called Breathing Time Bucket (BTB) [27] and a hybrid approach combined the above two were used for the simulation of a predator-prey model. The moderate optimistic approaches resulted in better performance. They did not employ a 3D grid geometry in their simulation.

XTW [28], an optimized version of TW, introduces a new optimistic synchronization mechanism to improve the performance of Time Warp. XTW consists of a new event scheduling algorithm, XEQ, and a new rollback mechanism, rb-message. XEQ has an  $O(1)$  cost bounded on the number of simulated entities (not on the number of events). Rb-message not only reduces the computing cost of annihilating previously sent messages, but also dramatically reduces the memory cost by eliminating the output queue in each LP. NTW inherits all of those features in XTW.

Without employing PDES, [21] developed the Lattice Microbes software to efficiently sample trajectories from either the Chemical Master Equation (CME) and Reaction Diffusion Master Equation (RDME) on a high performance computing infrastructure (workstation containing a Supermicro X9DRG-QF motherboard with dual Xeon E5-2640 CPUs and four GTX680 GPUs using NVIDIA drive), taking advantage of GPUs to increase performance. They employed a multiple thread approach to get efficient shared-memory communication between host threads, and avoided high GPU context switching overheads that would otherwise occur for multi-process access approach (i.e. with MPI). They considered uniform sub-volumes with some spacing and employed a multi-particle diffusion method. They use a dynamic load balancing to deal with inhomogeneous workloads. Employing a very small model (four reactions and 4 species), two and four GPUs provide a speedup over the single device, however for smaller volumes the benefit of four GPUs is correspondingly smaller. Eight GPUs did not provide any speedup when the sub-volume size was smaller than 64 cubic microns.

None of those above mentioned approaches employed a real neuronal geometry and did not employ a real model (e.g. calcium buffering, calcium wave model etc.) as a benchmark to verify their simulators. We use models derived from real NEURON models to verify NTW's correctness and to examine its performance.

### 2.3 Intra-cellular Calcium Signaling Pathways

A signaling pathway is initiated when a molecule activates a specific receptor located on the cell surface or on the inside of a cell. In turn, this receptor triggers a biochemical chain of events inside the cell which creates a response. Neurotransmitters transmit signals across a

synapse between two neurons. When a receptor on a post-synaptic neuron receives a neurotransmitter, it initiates intra-cellular signaling pathways. The role of  $Ca^{2+}$  signaling is very important to a neuron's response.

The basic mechanism of calcium signaling depends upon increases in the intra-cellular concentration of calcium ions. In most cells the concentration of intra-cellular calcium oscillates with a period ranging from a few seconds to a few minutes. These oscillations often take the form of waves. At rest, the concentration of calcium in the cell cytoplasm is low while outside the cell and in the internal compartments of the cell (e.g. the endoplasmic reticulum (ER)) it is high, as shown in figure 2. The ER acts as an internal warehouse of calcium ions from which calcium can exit to the cytosol through channels such as inositol triphosphate receptors,  $IP_3R$ , (e.g. it can also exit via RyR or leak). The  $IP_3Rs$  are located on the surface of the ER. Calcium ions,  $Ca^{2+}$ , can be pumped back from the cytosol to the ER by ATPase pumps.

When a postsynaptic neuron is electrically excited by receiving neurotransmitters at receptors, its voltage gated calcium channels (VGCC) located in the plasma membrane are opened and some calcium ions enter into the cytosol. This excitation also activates transmembrane proteins (a type of membrane protein spanning the width of the biological membrane to which it is permanently attached) to facilitate communication between cells by interacting with chemical messengers and G-proteins. G-proteins are a family of proteins involved in transmitting signals from stimuli coming from outside a cell to the inside of the cell. They function as molecular switches. The G-protein activates a Phospholipase C (PLC) enzyme and produces two second messengers, di-glyceride (DAG) which remain in the membrane and  $IP_3$ , which diffuses through the cytoplasm of the cell and binds to  $IP_3$  receptors ( $IP_3R$ ). When an  $IP_3R$  channel is triggered by both  $Ca^{2+}$  and  $IP_3$ , it is opened and allows the fast release of calcium from the ER to the cytoplasm, as shown in figure 2.

Typical calcium signaling pathways involve both binding and enzymatic reactions while molecules move through the intra-cellular space randomly. Hence binding and enzymatic reactions in combination with diffusion are the basic building blocks for modeling intra-cellular signaling pathways [4]. Recent intra-cellular calcium model consists of deterministic reaction-diffusion equations coupled to stochastic transitions of the calcium channels. The calcium and buffer concentrations in the cytosol are represented by partial differential equations (PDE). Stochastic quantities are the discrete states of channel units which determine the open/close state of a channel. The intra-cellular calcium concentration is determined by calcium diffusion, the transport of calcium ions through the ER membrane and the binding and unbinding of buffer molecules. The reaction terms, buffer binding and unbinding of calcium are modelled by the mass action kinetics in which the rate of a chemical reaction is proportional to the product of the concentrations of the reacting chemical species.

In a neuron calcium releases do not occur with a regular period, but are strongly influenced by stochastic process [13] [19]. The exact nature of these stochastic processes is not clear, but the most plausible explanation is that stochastic opening and closing of the  $IP_3R$  is the most important influence causing irregularity in the calcium release. In [30], the calcium

dynamics of a cell is formulated as a hybrid model in which the reaction-diffusion equations are used (a high concentration of calcium and buffers in the cytosol is assumed) and the opening/closing of channels is stochastic. In this paper we develop an  $IP_3R$  model and a stochastic simulation to predict the behavior of individual channels.

### 3 NEURON and NTW

NEURON [3] is a simulation environment which was primarily developed by Michael Hines at Yale. In this environment, complex nerve models can be created by connecting multiple one-dimensional sections together to form arbitrary neuron morphologies. NEURON also allows for the insertion of membrane properties in these sections (including channels, synapses, and ionic concentrations). In NEURON, the ion channels of axons and soma are typically of the Hodgkin-Huxley type [12]. NEURON is very flexible and supports a wide class of models.

The computation executed by the nervous system involves the spread and interaction of electrical and chemical signals within and between neurons and glia cells (a type of cell in the brain which supports neuronal communication and also plays a vital role in the development of human intelligence). Those signals can be modeled by the diffusion equation and the cable equation, which are partial differential equations in which the potential (voltage, concentration) and the flux (current, movement of a solute) are smooth functions of time and space. In NEURON, these partial differential equations are solved numerically by converting them into difference equations.

A deterministic reaction-diffusion model is not accurate [4] when a small number of  $Ca^{2+}$  ions are involved (e.g. a neuronal spine which is a small membranous bump on a neurons dendrite which typically receives input from a single synapse of an axon). Those quasi-isolated compartments like spines are so small and calcium concentrations are so low that one extra molecule diffusing in by chance can make a nontrivial difference in concentration (percentage-wise). These rare events can affect dynamics discretely in such way that it cannot be evaluated in a deterministic simulation. Stochastic models of such a system provide a more detailed understanding of these systems than existing deterministic models because they capture their behavior at a molecular level. A sequential version of NTW is already integrated with NEURON. The experimental integration of parallel NTW with NEURON is also done as to check its compatibility with NEURON. The interaction between NTW and NEURON is shown in figure 3.

Python has direct access to NEURON and can import NEURON's different computational modules by using the *import* statement. On the other hand, NTW's code is in C++ and Python does not have direct access to C++ code. However, Python can use ctypes, a foreign function interface module (included in Python 2.5 and above) which allows for the loading of dynamic libraries and calls C functions. Hence Python can provide information such as the geometry (i.e. neighbor informations for each sub-volume, species and reactions, sub-volume size, etc.) from the NEURON simulator to NTW through the C-C++ interface.



NTW is an individual module which interacts with NEURON using Python's ctypes interface. Hence prior to the parallel simulation, pointers to all of NEURON's data structures are sent to NTW. As a result NTW can access NEURON's data structures and can update NEURON's state for event (reaction or diffusion) processing. NTW can update NEURON states immediately when NTW process an events during the simulation.

## 4 NTW

We have designed and implemented a parallel discrete event simulator, NTW, to simulate 3D stochastic reaction-diffusion system. We use NEURON's front end as NTW's front end, making it possible for a group of chemical reactions to be input by the user. This enables the user to experiment with different reactions and different concentrations of molecules and ions as well as their associated reaction rates. It is also possible to experiment with different diffusion rates between adjacent cells.

NTW inherited the multi-level priority queue from XTW [28]. A history queue used to record scheduling history has been added. Every sub-volume (SV) in NSM is an LP in NTW. The reactions and the diffusion between sub-volumes are events in NTW.

### 4.1 Architecture

LPs are grouped together into clusters which, in turn, can be distributed among separate physical computational units. We currently allocate one cluster per core. Each cluster processes the events belonging to its LPs in increasing time-stamped order. There is a special cluster, called a controller, which is in charge of distributing the simulation workload, computing the Global Virtual Time (GVT): minimum time stamp among all unprocessed and partially processed messages in the system, and collecting the simulation results. We employ Matters algorithm [29] to calculate the GVT. Checkpointing is done upon the arrival of a diffusion event at a cluster. The architecture and communication overview of NTW is shown in figure 4.

In every cluster there are two event queues, the clEQ and the inputExtEQ. The clEQ is used to sort the events generated by local LPs (i.e. within the same cluster). Its top event is the lowest time stamped event of the cluster. All events from different clusters are temporarily put into inputExtEQ and then forwarded to an input channel event queue, ICEQ. The priority SV queue is a container of SVs. The head of the SV priority queue always points an SV of minimal local time of next event within the cluster.

In a three-dimensional geometry, an SV can have at most six adjacent SVs, i.e. neighbors. The structure of an SV is the result of this observation. Each SV has a SV event queue (SVEQ), input channel event queue (ICEQ) which is used to hold diffusion events from neighbors, a processed event queue (PEQ), a state saving queue (SQ) and a history queue (HQ). Readers who are interested in the details of multi-level queuing may turn to [28].

The history queue (HQ) is an addition to the structure described in XTW [28]. It can be viewed as an array of its neighbors, in which each element of the HQ stores the time stamp of the last event sent to the corresponding neighbor. The HQ is used when the SV has to be

rolled back. For example, suppose that the local virtual time of SV  $i$  is 100, its HQ[0] is 80 and HQ[1] is 90. Assume that SV  $i$  receives a straggler and is rolled back to a checkpoint at 88. After retrieving the local virtual time and recovering state it can send rb-messages. It is clear that a rollback-message (rb-message) should be sent to the neighbor defined by HQ[1] and does not need to be sent to the neighbor defined by HQ[0].

## 4.2 Event Flow

The event set in NTW consists of a rd-event, a diffusion-event and a rb-message event. When an LP receives an event message, it checks to see what sort of message it is. If the message is a straggler, the LP rollbacks. If it is a rb-message, events from input channel queue with time stamps greater than the rb-message's time stamp are removed. Otherwise the message is placed into the input channel queue. The algorithm is depicted in figure 5. When a cluster receives a diffusion event from an LP located in another cluster, it is placed in the inputExtEQ and then forwarded to the appropriate ICEQ.

The steps for processing events in SVs follow NSM approach in which rd-events are always scheduled to head of the SV priority queue whereas diffuse events are always scheduled to any neighbor (depending on random number) SVs, see figure 6.

## 5 Experimental Work and Analysis

$Ca^{2+}$  is an important second messenger signal in many cell types, with diverse roles, from fertilization to regulating gene expression [35]. It is of critical importance to neurons as it participates in the transmission of the depolarizing signal and contributes to synaptic activity [32].  $Ca^{2+}$  signaling waves in neurons were discovered more recently and is not yet fully understood however is thought to play an important role in synaptic transmission which is the form of secretion that leads to the release of neurotransmitters [32]. Nowadays, neuroscientists believe neuronal transmission has great impact in the process of learning and the formation and consolidation of memory [32].

Our experiments made use of two models - a calcium buffer [4] on a dendritic branch derived from NEURON simulation environment and a newly derived discrete event calcium wave model on a cylinder of 3D grid of sub-volumes cubes (derived from NEURON simulation environment) and on an one dimensional geometry.

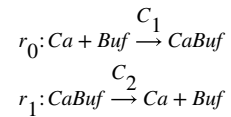
We make a comparison between a deterministic simulation in NEURON and a stochastic parallel simulation in NTW on a calcium buffer model to verify NTW's accuracy with respect to deterministic computation. We use the same reaction and diffusion rates, the same geometry (dendritic branch). We also employed the calcium buffer model to ascertain NTWs performance.

We use a discrete event calcium wave model derived from a deterministic model [35] [33].

### 5.1 Calcium Buffer Model

Free calcium,  $Ca^{2+}$ , is buffered by intra-cellular buffers (e.g. calmodulin or parvalbumin). It can escape from these buffers, resulting in an almost constant concentrations of cytosolic

calcium. This observation can be used to verify our simulator. The buffer model includes two reactions as follows:



Here, the reaction constant,  $C_1$ , for reaction  $r_0$  is  $0.01/\mu Mms$  and for reaction  $r_1$  the reaction constant,  $C_2$ , is  $0.01/ms$ . The diffusion constant of  $Ca$  is  $0.0001 \mu m^2/ms$ .  $Buf$  and  $CaBuf$  are not mobile species i.e. diffusion constant for those are 0.

The cylinder and branch are basic shapes for modeling neurites in NEURON. We use a dendritic branch geometry, also referred to as Y shaped, which is taken from a NEURON model. The Y-Shape geometry consists of three cylinders, each 10 microns long and 1 micron in diameter. Total volume of 3 connected cylinders is about  $23.56 \mu m^3$  and whole volume is sub-divided into 2766 sub-volumes. All sub-volumes are considered same in size and it is  $0.25 \times 0.25 \times 0.25$  cubic microns. Each cluster has near to the same number of SV's. The distribution of sub-volumes in a neuronal branch among the clusters is shown in figure 7.

**Hardware and Software Platform**—The simulation platform was an Intel(R) Core(TM) i7-3770S CPU with 4 physical cores (8 logical processors) and 16GB RAM Each core can execute 2 threads in parallel. Hence there are 8 logical processors. The operating system is Ubuntu 12.04, with kernel 3.2.0-29-generic-pae. The MPI version is (Open MPI) 1.4.3, gcc version is 4.6.4. NTW is implemented by C++.

Concentrations were recorded for both the deterministic and parallel stochastic algorithms - see figure 8 for different concentrations. We employed a Y-shape geometry with the same reaction and diffusion rates and obtained almost the same behavior for both simulations. In the high concentration experiment, the initial concentrations in NEURON model for Ca, Buf and CaBuf were  $8.0 \mu M$ ,  $4.0 \mu M$  and  $0.0001 \mu M$  respectively. In order to verify the accuracy of the parallel simulation, we kept the same configurations. The parallel version was run on four cores (one controller and three workers). The same experiment was done for low concentrations-  $0.8 \mu M$ ,  $0.4 \mu M$  and  $0.0001 \mu M$  for Ca, Buf and CaBuf respectively. The standard deviation plots for both the high and low concentration experiments are shown in figure 9.

To compare the results obtained by the NTW sequential (one controller with one worker) and parallel (one controller with several workers) stochastic simulations, we employed the calcium buffer model on the same Y-shape geometry. The NTW sequential and parallel (one controller with three workers) simulation with a standard deviation is shown in figure 10.

For all of the stochastic simulation experiments, the average of three parallel stochastic runs is considered. The standard deviation of three stochastic runs is shown in figure 11. The average standard deviation of the three stochastic runs (on 25 sample points) for Ca, Buf, and CaBuf are  $0.01 \mu M$ ,  $0.006 \mu M$  and  $0.095 \mu M$  respectively.

**Performance**—To measure the speedup of the parallel simulator, we employed a calcium buffer model on a neuronal branch and ran the parallel simulation for 5.7 virtual time units during which 1.2 million events were processed. The simulation took 2.53 seconds for one worker and for two workers it required 1.27 sec, as shown in the table 1.

The execution time and speedup plot for the calcium buffer model on the Y-shape geometry are portrayed in figure 12 and figure 13 respectively. When a dendrite branch is distributed over multiple logical processors, communication latency is created and the execution time flattens out at 7 logical processors.

The number of rollbacks increases linearly when the number of worker process increases, the result of increased communication between the workers. With proper load balancing we can distribute the communication workload over the processors and decrease the number of rollbacks.

## 5.2 Stochastic Discrete Event Calcium wave model: including $Ca^{2+}$ activating and $Ca^{2+}$ inhibiting sites dynamics

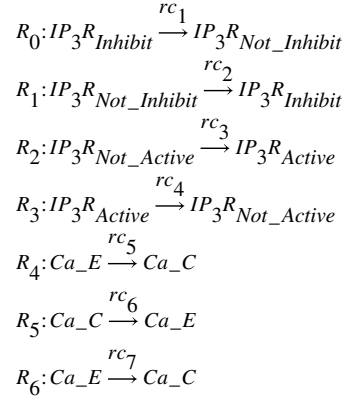
In the deterministic approach, the calcium concentration in the cytosol,  $[Ca_C]$ , is calculated at every time step from different (in and out) fluxes-  $J_{IP_3R}$ ,  $J_{SERCA}$ , and  $J_{LEAK}$  [35]. In the stochastic approach, different events (Channel Open, Release, Pump back and Leak) at discrete points of time are considered. The event frequency can be controlled by their (in/ out) flux rates, as derived in a mathematical model [35]. We have derived a stochastic reaction-diffusion discrete event calcium wave model from the deterministic model by considering only two bindings sites (activating and inhibiting Calcium sites). Because of the high occurrence of  $IP_3$  binding and unbinding [33] ignored the  $IP_3$  binding site in their  $IP_3R$  model. Parameter values were obtained from [35] to produce a calcium wave propagation in an unbranched one dimensional geometry (length of 200 micron and diameter of 1 micron). We also observe  $Ca^{2+}$  wave propagation in a cylinder with a diameter of 1 micron and a length of 20 micron which consists of 3D grid of 1701 sub-volumes.

**The stochastic channel dynamics of  $IP_3R$** —The  $IP_3R$  releases  $Ca^{2+}$  from the ER to the cytosol. It consists of four identical sub-units, each of which is composed of three binding sites [33]: an activating  $Ca^{2+}$  site, an inhibiting Ca site and an  $IP_3$  binding site. The three binding sites allow for eight different states  $X_{ijk}$  for each subunit. The index  $i$  stands for the  $IP_3$  site,  $j$  for the activating  $Ca^{2+}$  site, and  $k$  for the inhibiting  $Ca^{2+}$  site. An index is 1 if an ion is bound and 0 otherwise. Transition probabilities per unit time for transitions which involve the binding of a molecule are proportional to the concentration of that molecule. The channel is open if the subunit is in  $X_{110}$ , i.e., they have bound  $Ca^{2+}$  at the activating site and  $IP_3$ . Because the transition rates between the states  $X_{0JK}$  and  $X_{1JK}$  ( $IP_3$  binding and dissociation) are two orders of magnitude faster than the other transition rates [33] ignored the  $IP_3$  binding site. We also consider the same approach and assumed that the channel has a possibility of opening if the subunits is  $X_{10}$ .

The binding and dissociation of calcium  $Ca^{2+}$  at the activating and inhibition sites are stochastic events rendering the opening and closing of the channel a stochastic process. This stochastic process is coupled to the concentration of cytosolic calcium because the binding

probabilities per unit time depend on it and the number of open channels determines the concentration.

The transitions corresponding to reactions follow:



The first two reactions,  $R_0$  and  $R_1$ , correspond to  $Ca^{2+}$  binding and unbinding at the  $Ca^{2+}$  inhibition site.  $R_2$  and  $R_3$  are calcium binding and unbinding at the calcium activation site. Reaction  $R_4$  is for calcium release from ER to cytosol.  $R_5$  and  $R_6$  are for the Sarco/Endoplasmic Reticulum  $Ca^{2+}$ -ATPase (SERCA) pump from cytosol to ER and leaking  $Ca^{2+}$  to cytosol, respectively. Calcium in the cytosol is  $Ca\_C$  and calcium in the Endoplasmic Reticulum, ER, is  $Ca\_E$ . Two mobile species in this model are  $Ca\_C$ , for which the diffusion constant is  $D_C = 0.75 \mu m^2/ms$  and  $IP_3$ , for which the diffusion constant is  $D_{IP_3} = 1.75 \mu m^2/ms$ . We assume  $Ca\_E$  is not mobile, so its diffusion constant is,  $D_{CE} = 0$ .

In NSM, at every iteration, the reaction rates for all of the reactions are evaluated. In order to calculate a reaction rate, we follow the flux rate calculation of the deterministic model [35]. For experiment, the reaction constants were set as follows:  $rc_1 = 1.0$ ,  $rc_2 = 1.0$ ,  $rc_3 = 1.0$ ,  $rc_4 = 1.0$ ,  $rc_5 = 10.0$ ,  $rc_6 = 0.5$  and  $rc_7 = 1.5$ .

The calculation of NSM reaction rates are given below:

**Reaction rate for reaction  $R_0$  (to not inhibit  $IP_3R$ ) and  $R_1$  (to inhibit  $IP_3R$ )**

**Channel):** The rate of  $R_0$  reaction i.e. Ca not inhibiting rate =  $rc_1 * IP_3R_{Inhibit} * h_{inf}$

The rate of  $R_1$  reaction i.e. Ca inhibiting rate =  $rc_2 * IP_3R_{Not\_Inhibit} * (1 - h_{inf})$ .

Here,  $h_{inf} = K_{inh} / (K_{inh} + [Ca\_C])$ .

$[Ca\_C]$  is the local concentration of calcium in the cytosol.

Initially,  $IP_3R_{Inhibit} = 0$  and  $IP_3R_{Not\_Inhibit} = 4$  (as for 4 sub-units) which causes  $R_1$ 's reaction rate to be greater than the  $R_0$ 's reaction rate. That means initially that all of the channels are in an inhibited state i.e.  $X_{I1}$ . When the  $R_0$ 's reaction rate is greater than  $R_1$ 's rate the channel is in not in an inhibited state i.e.  $X_{J0}$ .

**Reaction rate for reaction  $R_2$  (to activate  $IP_3R$ ) and  $R_3$  (to inactivate  $IP_3R$** **Channel):** The rate of  $R_2$  reaction i.e. Ca activating rate =  $rc_3 * IP_3R_{Not\_Active} * (1-n_{inf})$ .The rate of  $R_3$  reaction i.e. Ca inactivating rate =  $rc_4 * IP_3R_{Active} * n_{inf}$ Here,  $n_{inf} = [Ca\_C] / (K_{Act} + [Ca\_C])$ Initially,  $IP_3R_{Not\_active} = 4$  and  $IP_3R_{Active} = 0$  which causes  $R_2$ 's reaction rate to be greater than  $R_0$ 's reaction rate. So all of the channels are in inactivate state i.e.  $X_{0K}$ . When  $R_3$ 's reaction rate becomes greater than  $R_2$ 's reaction rate, the channel becomes active i.e.  $X_{1K}$ .**Reaction rate for reaction  $R_4$  (to release  $Ca^{2+}$  from ER to cytosol):** The reaction rate of  $R_4$ , i.e. the Release rate =  $rc_5 * (J_{IP_3R})$ Here,  $J_{IP_3R} = V_{IP_3R} * x * n * m * h * ([Ca\_E] - [Ca\_C])$ 

Where,

$$n = IP_3R_{Active} / (IP_3R_{Active} + IP_3R_{Not\_Active})$$

$$m = IP_3 / (IP_3 + K_{IP_3})$$

$$h = IP_3R_{Not\_Inhibit} / (IP_3R_{Inhibit} + IP_3R_{Not\_Inhibit})$$

$$x = \text{number of } IP_3R \text{ channels per cluster.}$$

Here  $x = 1$  i.e. one  $IP_3R$  channel per cluster. $V_{IP_3R}$  and  $K_{IP_3R}$  are constants.It is notable that release depends on  $m$ ,  $n$ , and  $h$ .

- If  $IP_3$  is not available i.e.  $m = 0$  and release rate will be 0. This means release event will never happen.
- Similarly,  $h$  depends on  $IP_3R_{Not\_Inhibit}$ . When,  $IP_3R_{Not\_Inhibit}$  is 0 then  $h$  is also 0, which means that the channel is in an inhibited state and the release event cannot occur. The state of  $IP_3R_{Not\_Inhibit}$  or  $IP_3R_{Inhibit}$  is managed by reaction  $R_0$  and  $R_1$ .
- $n$  depends on  $IP_3R_{Active}$ . When,  $IP_3R_{Active}$  is 0 then  $n$  is also 0. This means  $IP_3R$  is in an Ca inactivated state. The value of  $IP_3R_{Active}$  and  $IP_3R_{Not\_Active}$  is always updated by reaction  $R_2$  and  $R_3$ .

**Reaction rate for reaction  $R_5$  (to pump back  $Ca^{2+}$  from cytosol to ER):** The reaction rate or pumping rate =  $rc_4 * J_{SERCA}$ Here,  $J_{SERCA} = V_{SERCA} * ([Ca\_C]^2 / (K_{SERCA}^2 + [Ca\_C]^2))$ .and  $V_{SERCA}$  and  $K_{SERCA}$  are constants.

**Reaction rate for reaction  $R_6$  (leak Ca from ER to cytosol):** The reaction rate i.e., the leak rate =  $rc_5 * J_{LEAK}$ .

Here,  $J_{LEAK} = V_{Leak} * ([Ca_E] [Ca_C])$ .

and  $V_{Leak}$  is a constant.

All constants are taken from deterministic model [35] are shown in table 2.

### 5.3 Propagation of Calcium Wave

Figure 14 shows a calcium wave through an array of sub-volumes, each of which has only one  $IP_3R$  receptor. When (1) there is a small number of  $Ca^{2+}$  and  $IP_3$  ions are available (2) the calcium activated site being activated and no calcium inhibition, the  $IP_3R$  channel releases  $Ca^{2+}$  from the ER to the cytosol, creating a small calcium wave called a ‘blip’. Several blips in a  $IP_3R$  cluster creates a ‘puff’. Because each cluster has only one  $IP_3R$ , we do not distinguish between blips and puffs in our experiments. Due to the puffs, the cytoplasmic calcium concentration is raised as shown in figure 14. The released calcium then diffuses to neighboring sub-volumes and activates nearby  $IP_3R$  via “calcium induced calcium release” (CICR). Thus a global propagation of a calcium wave is evoked, figure 14. In short,  $Ca^{2+}$  release at one  $IP_3R$  can trigger  $Ca^{2+}$  release at adjacent  $IP_3R$  via CICR, leading to the generation of  $Ca^{2+}$  waves.

**Model verification and wave propagation—**In order to observe wave propagation experimentally, we employed an array of two hundred  $1 \times 1 \times 1$  cubical micron SVs connected linearly as shown in figure 15. In every sub-volume we modeled the cytosolic and endoplasmic reticulum compartments by using a fractional volume for each, as shown in figure 1.

Initial concentration for both  $Ca^{2+}$  and  $IP_3$  are  $0.0033 \mu M$  (i.e. 2  $Ca^{2+}$  molecules per SV) and  $0.0 \mu M$  respectively. After a period of time, the concentration of  $IP_3$  is increased to  $0.332 \mu M$  (i.e. 200  $IP_3$  molecules per SV) in the middle six SVs (i.e.  $SV_{97}$  to  $SV_{102}$ ) and observed the spreading of a Ca wave as shown in figure 16. Similarly to observe the spreading of calcium wave through a 3D grid, we employed a cylinder with a diameter of 1 micron and a length of 20 micron which consists of 3D grid of 1701  $0.25 \times 0.25 \times 0.25$  cubical micron sub-volumes. Initial concentration for both  $Ca^{2+}$  and  $IP_3$  are  $0.0033 \mu M$  (i.e. 2  $Ca^{2+}$  molecules per SV) and  $0.0 \mu M$  respectively. After a period of time, the concentration of  $IP_3$  is increased to  $106.27 \mu M$  (i.e. 1000  $IP_3$  molecules per SV) in the middle nine SVs (i.e.  $SV_{845}$  to  $SV_{853}$ ) and observed the spreading of calcium through a 3D grid cylinder as shown in figure 17.

Because there is high concentration of  $IP_3$  in  $SV_{97}$  to  $SV_{102}$ , the release event can only occur at those SVs.  $IP_3$ , and then spread gradually along the dendrite, resulting in a  $Ca^{2+}$  activation of the  $IP_3$  receptors ( $IP_3Rs$ ). Activation of  $IP_3Rs$  permit release of  $Ca^{2+}$  from the endoplasmic reticulum stores into the cytosol. This causes the concentration of calcium in cytosol,  $[Ca_C]$  to increase and to start to diffuse in both directions (left and right) from the middle and to affect the neighbor SVs as well. In addition the  $IP_3$  also diffuses to neighbors

and causes neighboring SVs to start to release events. Thus a global wave of calcium in the cytosol,  $Ca_C$ , starts to propagate in both directions with respect to time (1 ms to 30 ms) as shown in figure 16. The calcium wave is travelling very fast (about 3.3 micron per ms), which is far from a real biological neuron (1 micron every 20 ms). In fact we reproduced the qualitative dynamics and moved on because we are interested in the performance of NTW with our discrete model.

**Steady state  $IP_3R$  channel dynamics**—We developed an  $IP_3R$  model and a stochastic simulation to predict the behavior of individual channels. The  $IP_3R$  model plays a central role not only for the understanding of channel kinetics but also as a building block for constructing larger scale models of cellular calcium signaling. Figure 18 describes the dependence of  $IP_3R$  channel open probability ( $P_o$ ) as a function of cytosolic  $Ca^{2+}$  for different concentration of  $IP_3$ .

Experiment: Initially all channels of the domain (sub-volume  $SV_0$  to  $SV_{199}$  each of which has only one  $IP_3R$  channel) are closed. The concentration of  $Ca^{2+}$  in cytosol is .0033 uM and the concentration of the  $IP_3$  in cytosol is 0 uM. After a very short period of time, the concentration of  $IP_3$  (for all SVs) rises to .0083 uM. This causes all of the  $IP_3R$  channels to open and increases the level of  $Ca^{2+}$  concentration in the cytosol very sharply. When  $Ca^{2+}$  concentration in cytosol is reached into a certain point, here it is .035 uM, all channels starts to close and reach into a steady state.

Open probability ( $P_o$ ) calculation: The NSM algorithm first calculates the total reaction and diffusion rates at every iteration. Then it decides whether the event is reaction or diffusion event randomly. If the event is a reaction, NSM selects a reaction out of the 7 reactions. The model consists of 7 reactions,  $R_0$  to  $R_6$ , where  $R_4$  is the open reaction i.e. release  $Ca^{2+}$  from ER to cytosol. The open probability  $P_o$  is defined as the ratio of the total number of  $R_4$  reactions occurring (release events),  $N_{R4}$  to the total number of reaction events, N.  $P_o = N_{R4}/N$ . Figure 18 is the plot of  $P_o$  for different concentration levels of cytosolic calcium with 3 different concentrations of  $IP_3$ .

[34] experimentally observed that the channel open probability is a bell-shaped function of the concentrations of calcium in cytosol,  $[Ca_C]$ . The open probability varies with respect to  $IP_3$  concentrations. We also obtained the same behavior, validating our stochastic discrete event calcium wave model. It is notable that when calcium concentration is about .073  $\mu M$  the open probability is very low (less than .02). In a stochastic simulation, the channel open probability  $P_o$  never goes to zero as in steady state some releases do occur.

**Performance**—The execution time of our model in the neuronal branch geometry is displayed below in figure 19. We first note that it takes 5 worker processes for the execution time of the model to be divided in half. In the Calcium buffer model it took 2 workers to achieve this.

The reason for this has to do with the large computational imbalance between the areas in the model with high calcium (covered areas) and those with low calcium (uncovered areas).



This imbalance results in a large number of rollbacks—they increase almost linearly with the number of process—see figure 20 and degrade the performance of the simulation.

Our experiments clearly revealed this computational imbalance. Table 3 shows experimental data comparing the workloads of the covered and uncovered areas.

### Some take-away from these experiments

- 95% more events are processed in the covered area than in the uncovered area. Among the processed events in the covered area about 15% are reaction events and about 85% are diffusion events. We conclude that it is important to detect the covered area in order to determine the proper distribution of sub-volumes among the worker processes.
- The size of the covered area increases with time, so dynamic load balancing is worthwhile investigating.
- The rate of spreading of the covered area depends on the speed of calcium wave which in turn depends on the concentration of  $IP_3$ . If the concentration of  $IP_3$  is high, the Ca wave spreads quickly, otherwise slowly [35]. Hence we can detect the covered area via the concentration of  $IP_3$  in the SVs.

We intend to explore the utility of a load balancing algorithm for this problem.

## 6 Conclusion

This paper describes a parallel simulation environment for a stochastic reaction-diffusion model, Neuron Time Warp (NTW). NTW was built as part of the NEURON project ([www.neuron.yale.edu](http://www.neuron.yale.edu)) and has been experimentally integrated with NEURON. Deterministic models for the chemical activity of a neuron have existed for some time, but cannot portray chemical behavior in a neuron when there are a small number of molecules involved in both the reactions and diffusion of these molecules. Stochastic models do provide us with a more detailed view. The reason for developing a parallel simulation is to be able to simulate a larger part of a neuron or a network of neurons in some detail.

We made use of NTW for two models in this paper, a calcium buffer model and a calcium wave model. The calcium buffer model was used primarily to compare the behavior of NTW to that of a deterministic model as a means to verify NTW. The calcium wave model, on the other hand, is intended to investigate the behavior of a calcium wave which plays an important role transmission in a neuron. We developed a discrete event calcium wave model with diffusible  $IP_3$ , diffusible  $Ca^{2+}$ ,  $IP_3$  receptors ( $IP_3R$ ), endoplasmic reticulum (ER)  $Ca^{2+}$  leak and an ER pump (SERCA). Our results indicated that the bulk of the computation moves with the spreading of the actual wave.

We are in the process of developing a load balancing algorithm for NTW. This is a topic of vital importance for the simulation of networks of neurons which contain hundreds of thousands or indeed millions of sub-volumes, i.e. large-scale realistic models. We intend to make use of techniques from artificial intelligence to build these algorithms similar to the ones described in [31]. We are combining the load-balancing algorithms with a window-

control algorithm which reduces the number of rollbacks, as in [31]. The load balancing/window control algorithms described in [31] were used in the context of parallel gate level simulation of VLSI circuitry. We are planning to explore the use of sub-volumes with different shapes and sizes which are connected in arbitrary ways in order to better accommodate different neuronal morphologies and models.

We end this paper with the proverbial view from 10,000 feet. NTW relies on the decomposition of a model into sub-models (sub-volumes in this paper, LPs in general) in order to effect a parallel simulation. This approach can also be made use of in the field of systems biology in order to create a realistic cell simulation. We should note that realistic cell simulation is one of the major goals of systems biology. Differential equation models can be used for part of a model and discrete event models can be used for other parts, depending on the desired level of detail. Either or both of these models can be executed in parallel.

## Glossary

<b>diffusion-event</b>	One type of NTW events. When rd-event does as a diffusion event it generates a diffuse-event which is forwarded to a neighbor sub-volume.. 5
<b>rb-message</b>	It is a notification message from a rolled back LP to neighbor LPs so that neighbor LPs are being corrected.. 5
<b>rd-event</b>	One type of NTW events which may occur reaction or diffusion.. 5
<b>rollback</b>	When a straggler message arrives, a rollback to the time stamp of the straggler is performed and all of processed events with a greater time stamp than that of the straggler are re-executed.. 5
<b>speedup</b>	Speedup is defined as the ratio of the sequential execution time to the parallel execution time.. 7
<b>straggler</b>	A late arrival event message into a logical process is referred as straggler.. 5

## ACRONYMS

<b>cIEQ</b>	Cluster Event Queue. 5
<b>GVT</b>	Global Virtual Time. 5
<b>LP</b>	Logical Process. 3
<b>NSM</b>	Next Sub-volume Method. 1, 2
<b>NTW</b>	Neuron Time Warp. 1, 2

**PDES** Parallel Discrete Event Simulation. 1, 2

## References

1. Azevedo FA, Carvalho LR, Grinberg LT, Farfel JM, Ferretti RE, Leite RE, Jacob Filho W, Lent R, Herculano-Houzel S. Equal numbers of neuronal and nonneuronal cells make the human brain an isometrically scaled-up primate brain. *Journal of Comparative Neurology*. 513(5):532–541.2009; [PubMed: 19226510]
2. Patoary, Mohammad Nazrul Ishlam; Tropper, Carl; Lin, Zhongwei; McDougal, Robert; Lytton, William W. Neuron time warp. *Proceedings of the 2014 Winter Simulation Conference*; December 2014; NJ, USA: IEEE Press; 3447–3458.
3. Hines, ML, Carnevale, NT. *The NEURON Book*. UK: Cambridge University Press; 2006.
4. Sterratt, D, Graham, B, Gillies, A, Willshaw, D. *Principles of Computational modeling in Neuroscience*. UK: Cambridge University Press; 2011.
5. Gillespie, DT. *The Journal of Physical Chemistry*. Vol. 81. USA: 1977. Exact stochastic simulation of coupled chemical reactions; 23402361
6. Gibson, MA, Bruck, G. *The Journal of Physical Chemistry A*. Vol. 104. USA: 2000. Efficient exact stochastic simulation of chemical systems with many species and many channels; 18761889
7. Gillespie, DT. *Journal of Chemical Physics*. Vol. 115. USA: AIP Publishing; 2001. Approximate accelerated stochastic simulation of chemically reacting systems.
8. Cao, Y, Li, H, Petzold, L. *The Journal of Chemical Physics*. Vol. 121. USA: AIP Publishing; 2004. Efficient formulation of the stochastic simulation algorithm for chemically reacting systems; 4059–4067.
9. Takahashi, K, Kaizu, K, Hu, B, Tomita, M. *Bionformatics*. Vol. 6. UK: Oxford University Press; 2004. A multi-algorithm, multi-timescale method for cell simulation; 538–546.
10. Leach, AR. *Molecular modeling: Principles and Applications*. USA: Prentice Hall; 2001.
11. Elf J, Ehrenberg M. Spontaneous separation of bi-stable biochemical systems into spatial domains of opposite phases. *System Biology (Stevenage)*, IEEE Proceeding. 1(2):230–236.
12. Hodgkin AL, Huxley AF. A quantitative description of membrane current and its application to conduction and excitation in nerve. *Journal of physiology*. 117:500–544.1952; [PubMed: 12991237]
13. Marchant J, Parker I. Role of elementary  $Ca^{2+}$  puffs in generating repetitive  $Ca^{2+}$  oscillations. *EMBO J*. 20:65–71.2001; [PubMed: 11226156]
14. Blackwell KT. Approaches and tools for modeling signaling pathways and calcium dynamics in neurons. *Journal of neuroscience methods*. 220(2):131–140. Nov 15; 2013 [PubMed: 23743449]
15. Bartol TM Jr, Land BR, Salpeter EE, Salpeter MM. Monte Carlo simulation of miniature endplate current generation in the vertebrate neu-romuscular junction. *Biophysical Journal*. 59(6):1290–1307. Jun; 1991 [PubMed: 1873466]
16. Andrews, Steven S; Addy, Nathan J; Brent, Roger; Arkin, Adam P. Detailed simulations of cell biology with Smoldyn 2.1. *PLoS Comput Biol*. 6(3):e1000705. Mar 12. 2010 [PubMed: 20300644]
17. Byrne, Michael J; Neal Waxham, M; Kubota, Yoshihisa. Cellular dynamic simulator: an event driven molecular simulation environment for cellular physiology. *Neuroinformatics*. 8(2):63–82. Jun; 2010 [PubMed: 20361275]
18. Hepburn, Iain; Chen, Weiliang; Wils, Stefan; De Schutter, Erik. STEPS: efficient simulation of stochastic reaction-diffusion models in realistic morphologies. *BMC systems biology*. 6:36. May 10. 2012 [PubMed: 22574658]
19. Falcker M. On the role of stochastic channel behavior in intra-cellular  $Ca^{2+}$  dynamics. *Biophys J*. 84:42–56. 2003; [PubMed: 12524264]
20. Chamakuri, N, Sten, R. *Journal of Computational Interdisciplinary Sciences*. Vol. 3. Pan-American Association of Computational Interdisciplinary Sciences; 2012. Whole-cell simulations of hybrid stochastic and deterministic calcium dynamics in 3D geometry; 3–18.

21. Hallock, Michael J, Stone, John E, Roberts, Elijah; Fry, Corey; Luthey-Schulten, Zaida. *Journal of Parallel Computing*. Vol. 40. USA: Elsevier B.V; 2014. Simulation of reaction-diffusion processes over biologically relevant size and time scales using multi-GPU workstations; 86–99.
22. Jeschke, M; Ewald, R; Park, A; Fujimoto, R; Uhrmacher, AM. *Parallel and Distributed Spatial Simulation of Chemical Reactions*. 22nd Workshop on Principles of Advanced and Distributed Simulation; IEEE; 2008. 51–59.
23. Dematte, L; Mazza, T. On parallel stochastic simulation of diffusive systems. *Proceeding of the 6th International Conference on Systems Biology*; Germany: Springer; 2008. 191–200.
24. Wang, B; Yao, Y; Hou, B; Peng, S. Experimental analysis of optimistic synchronization algorithms for parallel simulation of reaction-diffusion systems. *International Workshop on High Performance Computational Systems Biology*; Trento, Italy. 2009. 91–1001.
25. Wang, B, Yao, Y, Hou, B, Peng, S. *Computational Biology and Chemistry*. Vol. 35. Washington, DC, USA: IEEE Computer Society; 2011. Abstract Next Subvolume Method: A logical process-based approach for spatial stochastic simulation of chemical reactions; 5193–198.
26. Jefferson, David R. Virtual time. *ACM Trans Program Lang Syst*. 7(3):404–425.1985;
27. Steinman JS. SPEEDES: Synchronous Parallel Environment for Emulation and Discrete Event Simulation. *SCS Western Multiconference on Advances in Parallel and Distributed Simulation (PADS91)*. 23:95–103.1991;
28. Xu, Q; Tropper, C. XTW, a parallel and distributed logic simulator. 26th Workshop on Principles of Advanced and Distributed Simulation; ACM/IEEE/SCS; 2005. 181–188.
29. Friedemann Mattern. Efficient Algorithms for Distributed Snapshots and Global Virtual Time Approximation. *Journal of Parallel and Distributed Computing*. 18(4)1993;
30. Chamakuri N, Sten R. Whole-cell simulations of hybrid stochastic and deterministic calcium dynamics in 3D geometry. *Journal of Computational Interdisciplinary Sciences*. 3(1–2):3–18.2012;
31. Meraji, Sina; Zhang, Wei; Tropper, Carl. On the Scalability and Dynamic Load-Balancing of Optimistic Gate Level Simulation. *IEEE TRANSACTIONS ON COMPUTER-AIDED DESIGN OF INTEGRATED CIRCUITS AND SYSTEMS*. 29(9):1368–1380.2010;
32. Brini, Marisa; Cali, Tito; Ottolini, Denis; Carafoli, Ernesto. Neuronal calcium signaling: function and dysfunction. *Cellular and Molecular Life Sciences*. 71:27872814.Aug.2014
33. Falcke, Martin. *Biophysical Journal*. Vol. 84. Biophysical Society; 2003. On the Role of Stochastic Channel Behavior in Intra-cellular  $Ca^{2+}$  Dynamics; 4256
34. Shuai, Jianwei; Pearson, John E, Kevin Foskett, J, Mak, Don-On Daniel; Parker, Ian. *Biophysical Journal*. Vol. 93. Biophysical Society; 2007. A Kinetic Model of Single and Clustered  $IP_3$  Receptors in the Absence of  $Ca^{2+}$  Feedback; 1151–1162.
35. Neymotin, Samuel A, McDougal, Robert A, Sherif, Mohamed A, Fall, Christopher P, Hines, Michael L, Lytton, William W. *Neural Computation*. Vol. 27. MIT press; 2015. Neuronal calcium wave propagation varies with changes in endoplasmic reticulum parameters: a computer model; 898–924.

## Biographies

**Mohammad Nazrul Ishlam Patoary** is a Ph.D. student of School of Computer Science at McGill University. His research area is parallel discrete event simulation.  
mohammad.patoary@mail.mcgill.ca

**Carl Tropper** is a Professor in the Department of Computer Science at McGill University. His focus over the past several years has been on applying PDES techniques to stochastic discrete event simulations of neurons. His group has developed Neuron Time Warp.  
carl@cs.mcgill.ca.

**Robert A. McDougal** is a Postdoctoral Fellow in Neuroscience at Yale University with a PhD in Mathematics from The Ohio State University and an MS in Computational Biology

and Bioinformatics from Yale University. He is a developer for the NEURON simulator and for the SenseLab collection of neuroscience databases. His research focuses on developing computational techniques to study the brain. robert.mcdougal@yale.edu.

**Zhongwel Lin** is a Ph.D. student of College of Computer at National University of Defense Technology. He received M.S. degree in Computer Science and Technology from National University of Defense Technology. His research area is High Performance Simulation. zwlin@nudt.edu.cn.

**William Lytton** is an MD trained at Harvard, Columbia, Alabama, Johns Hopkins, UCSD and Salk Institute. He is a neurologist caring for the indigent at Kings County Hospital, and teaching and researching computational neuroscience at Downstate Medical Center, both in Brooklyn, NY. He is the author of “From Computer to Brain,” a basic introduction to computational neuroscience. His research involves the understanding of single-cell and network dynamics with application to neurological and psychiatric disease including epilepsy, stroke and schizophrenia. A major goal of his laboratory (<http://it.neurosim.downstate.edu>) is the eventual development of personalized medicine through drugs or devices that can be specifically designed to alter functional neurodynamics in the individual patient billl@neurosim.downstate.edu.

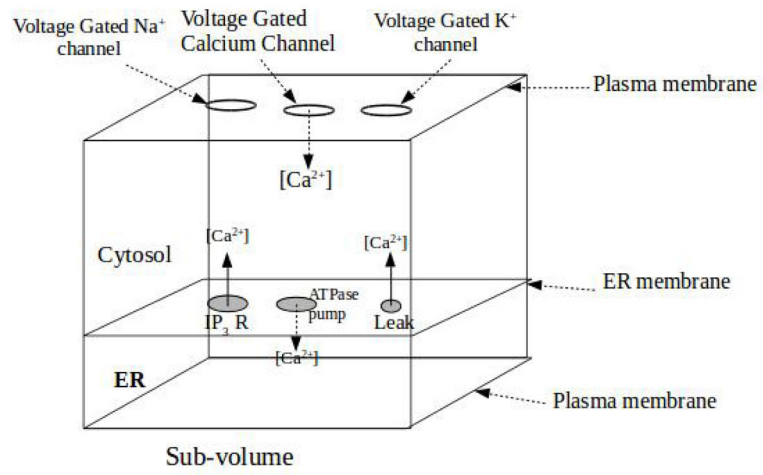


**Fig. 1.**  
Computational sub-volume domain for neuron.

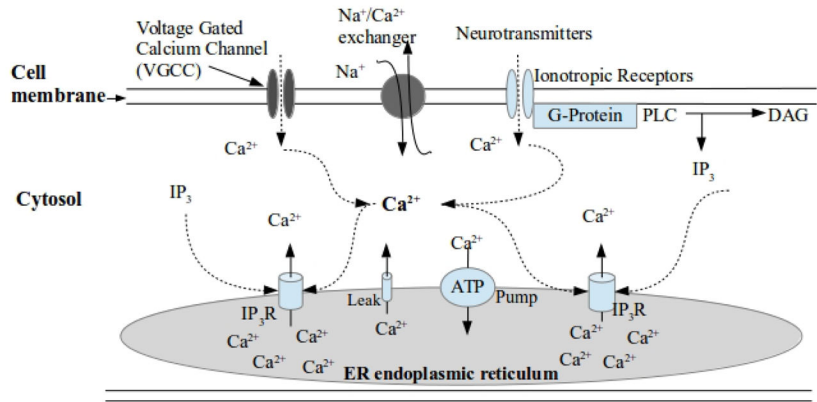


**Fig. 2.**  
Calcium wave signaling in neuron.

Author Manuscript

Author Manuscript

Author Manuscript

Author Manuscript

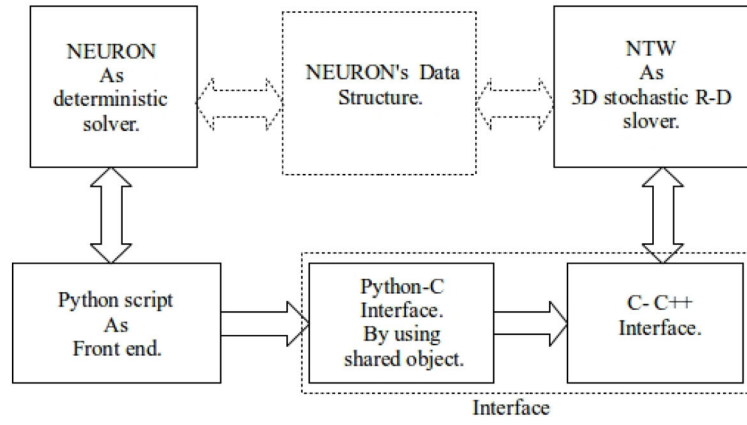


**Fig. 3.** Typical interaction between NEURON and NTW.



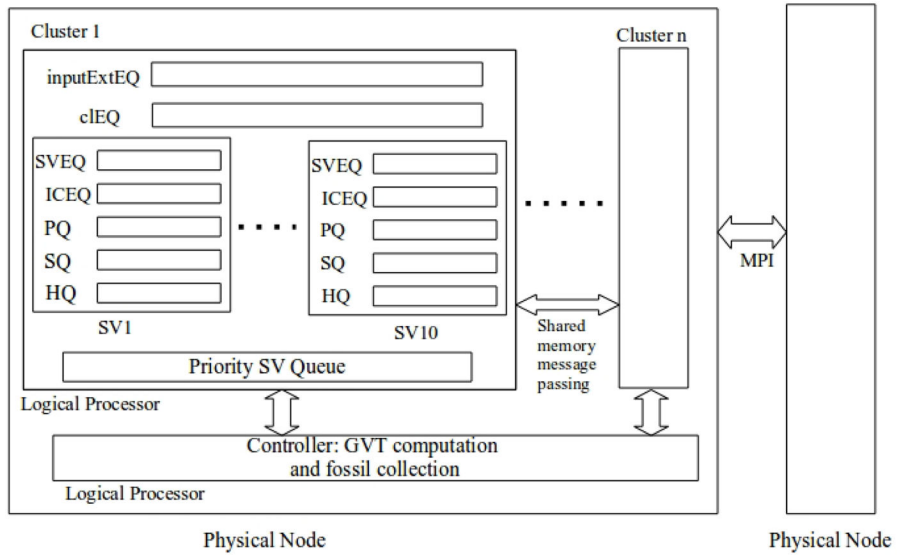


**Fig. 4.**  
The architecture and communication overview of NTW.

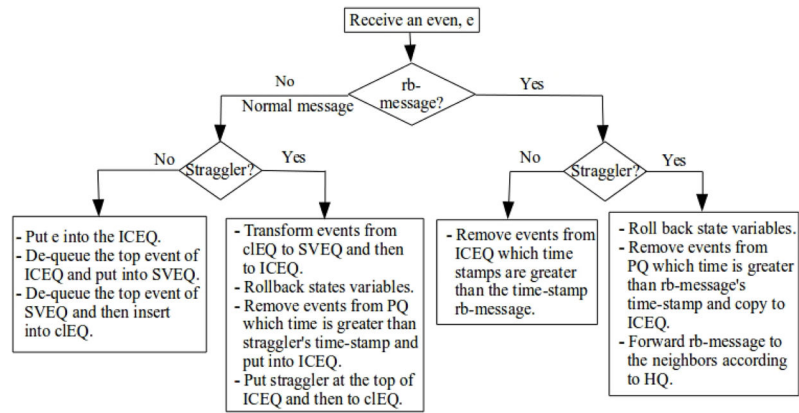


**Fig. 5.**  
LP level event receiving.

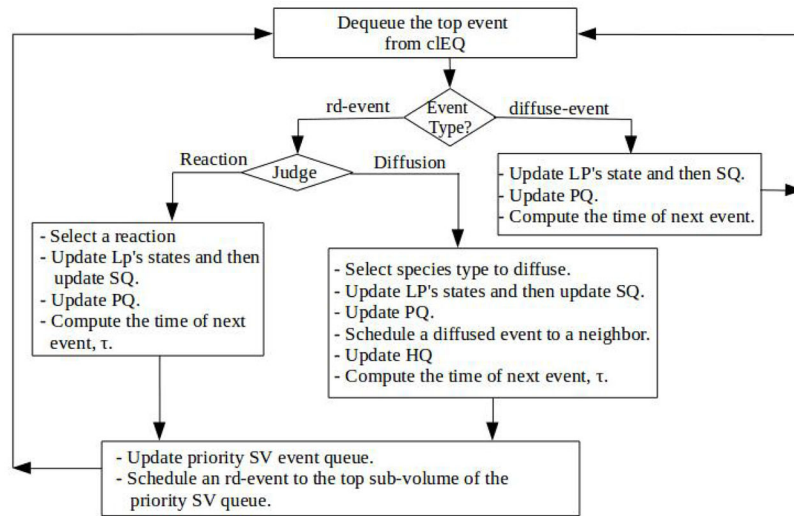


**Fig. 6.**  
Cluster level event processing.

Author Manuscript

Author Manuscript

Author Manuscript

Author Manuscript

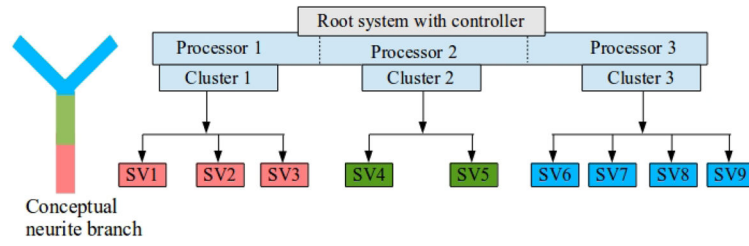


**Fig. 7.**  
 Conceptual partitioning of SVs of neuronal branch among the processes.

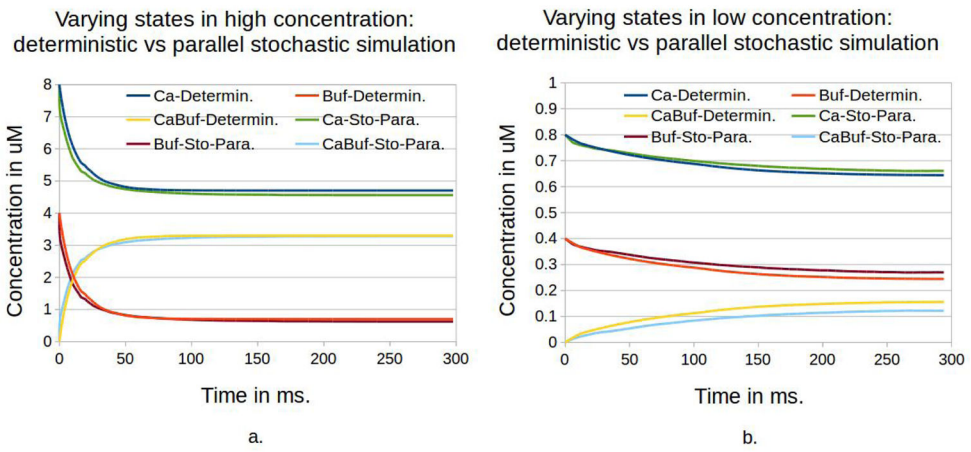


**Fig. 8.** Varying concentration in deterministic and parallel stochastic simulation for a. high concentration b. low concentration.

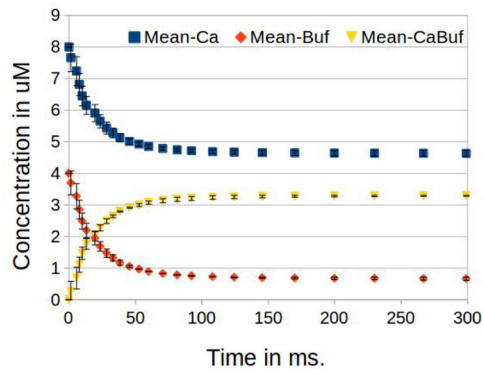
Author Manuscript

Author Manuscript

Author Manuscript

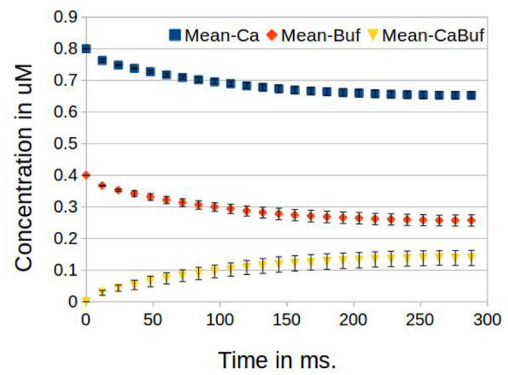
Author Manuscript

Standard deviation with high concentration:  
deterministic vs parallel stochastic simulation



a.

Standard deviation in low concentration:  
deterministic vs parallel stochastic simulation



b.

**Fig. 9.** Standard deviation between deterministic and parallel stochastic for a. high concentration b. low concentration.

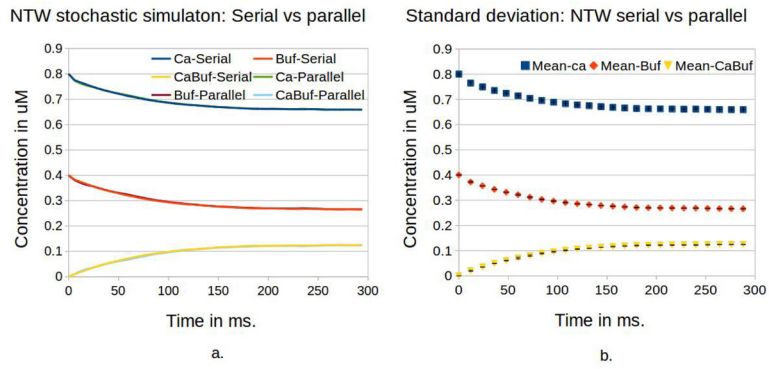


**Fig. 10.**  
a. Varying concentration in NTW stochastic sequential and parallel simulation. b. Corresponding standard deviation plot.

Author Manuscript

Author Manuscript

Author Manuscript

Author Manuscript

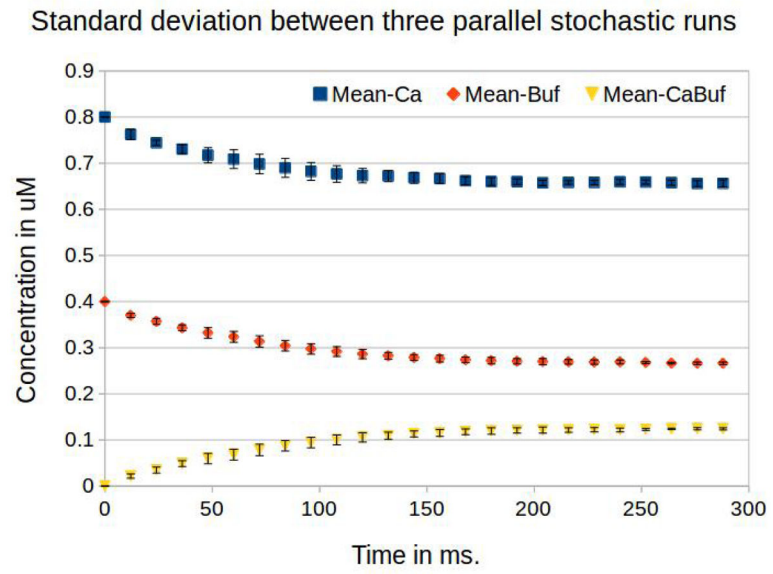


**Fig. 11.** Standard deviation of three parallel stochastic runs.

Author Manuscript

Author Manuscript

Author Manuscript

Author Manuscript



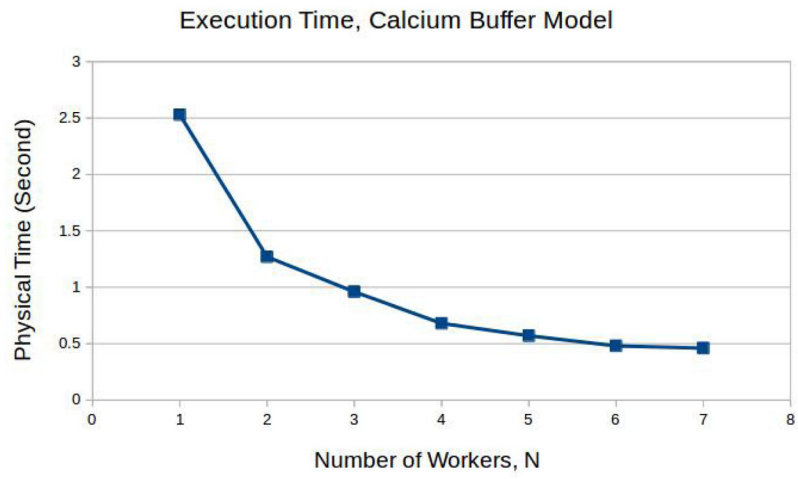


**Fig. 12.** Execution time of calcium buffer model in parallel simulation.

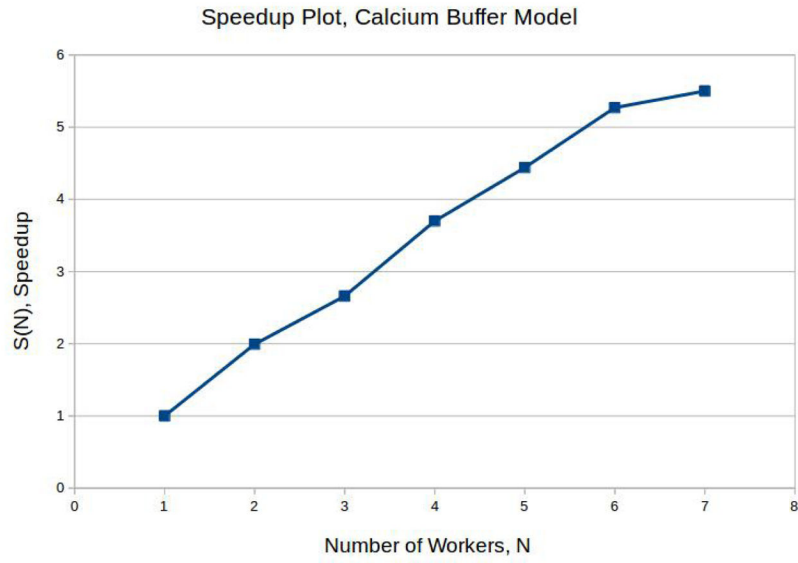


**Fig. 13.**  
Speedup of NTW as a function of number of worker process.

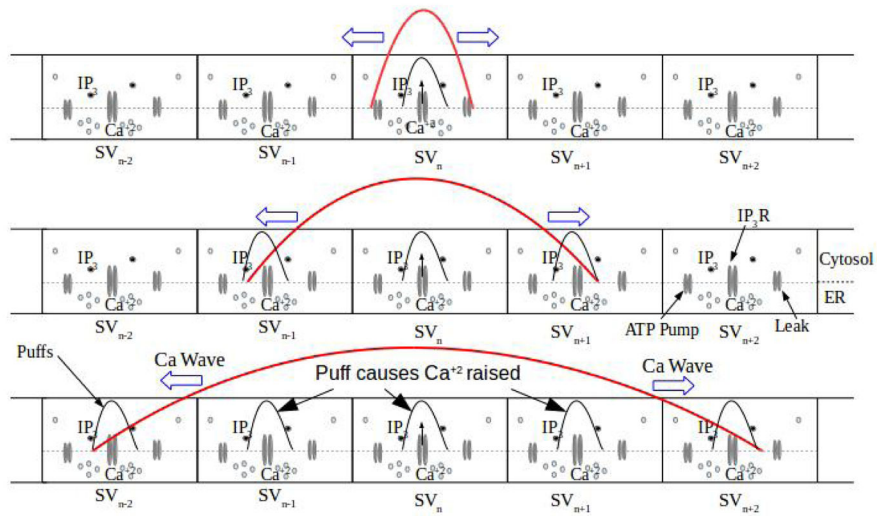


**Fig. 14.** Calcium wave propagation through a linear geometry with one  $IP_3R$  channel per micron.

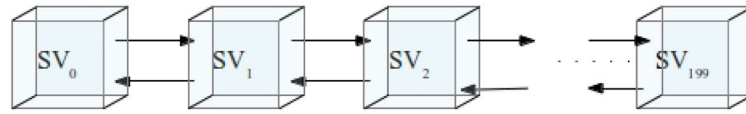


**Fig. 15.**  
Linear connection of computational sub-volumes, SVs.

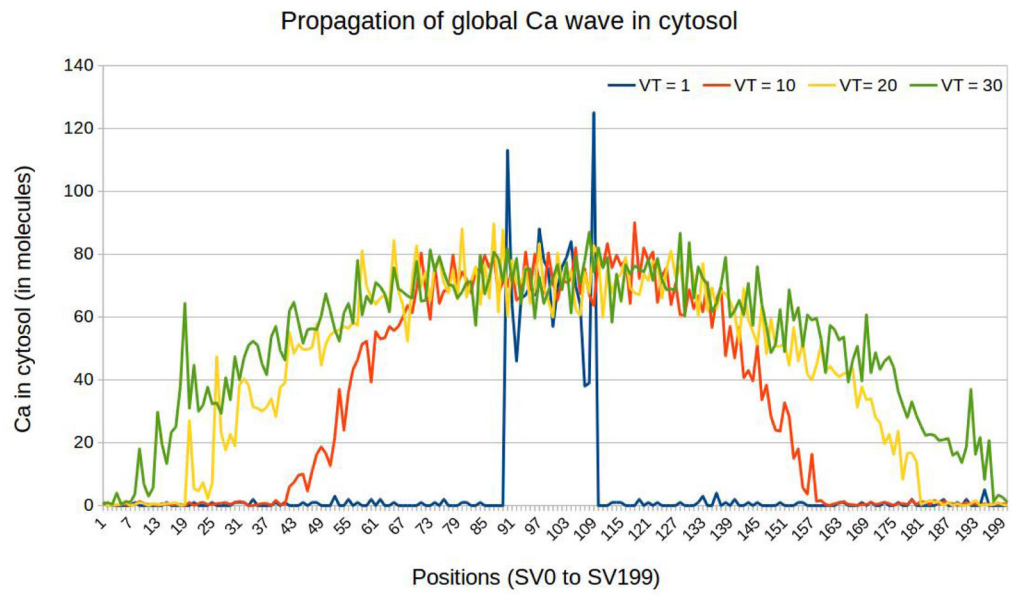


**Fig. 16.** Observation of calcium wave propagation in linear geometry.

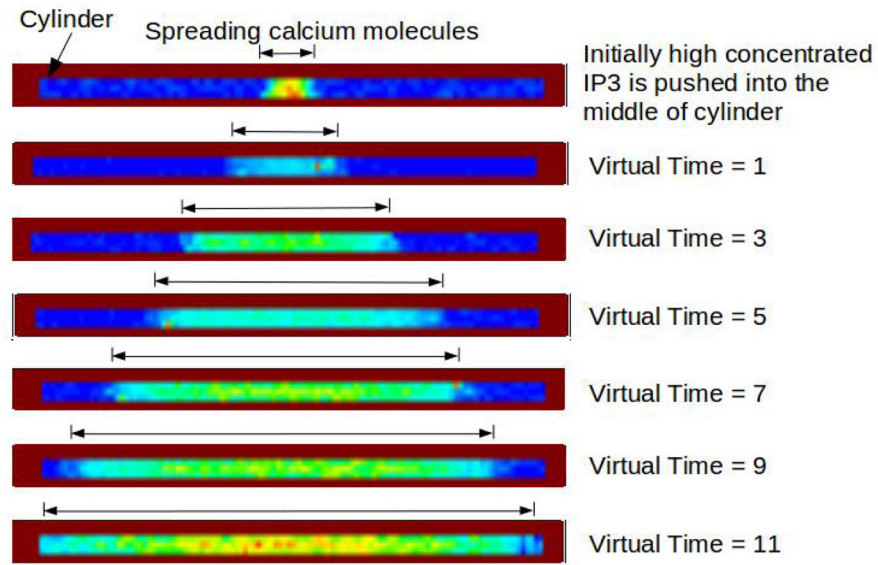


**Fig. 17.** Observation of calcium wave propagation in a cylinder with a diameter of 1 micron and a length of 20 micron which consists of 3D grid of 1701 sub-volumes.

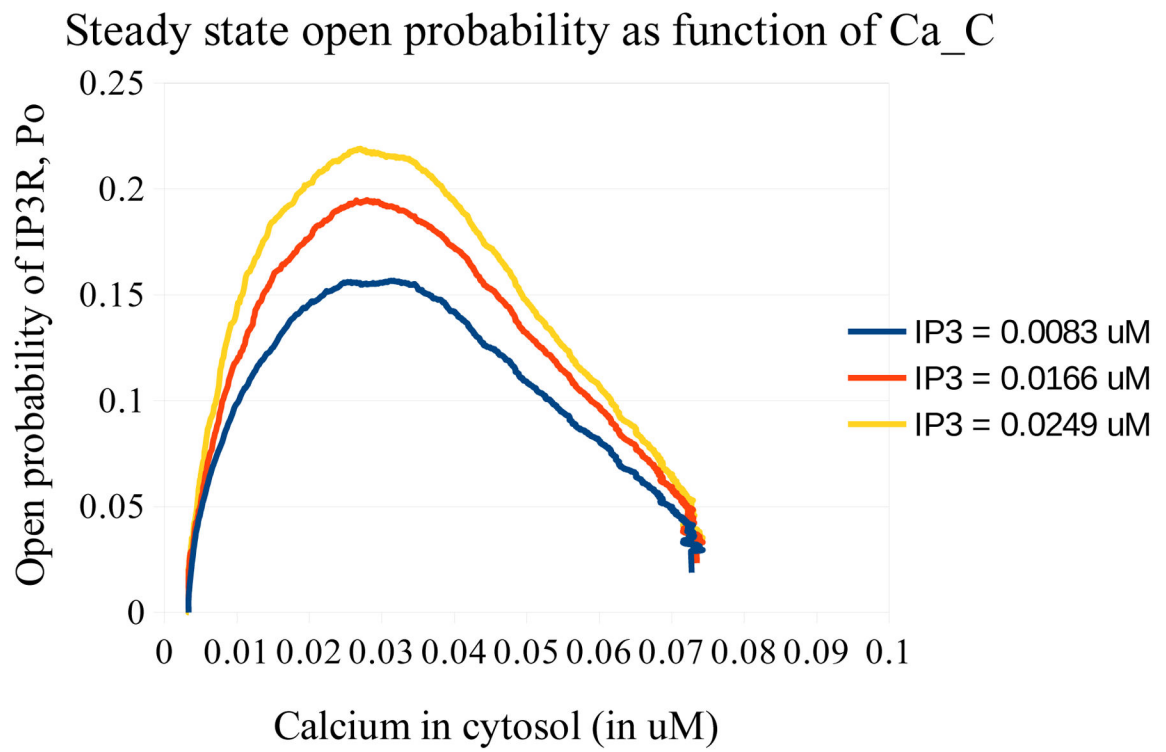


**Fig. 18.** Steady state open probability as function of calcium in cytosol,  $Ca_C$ .

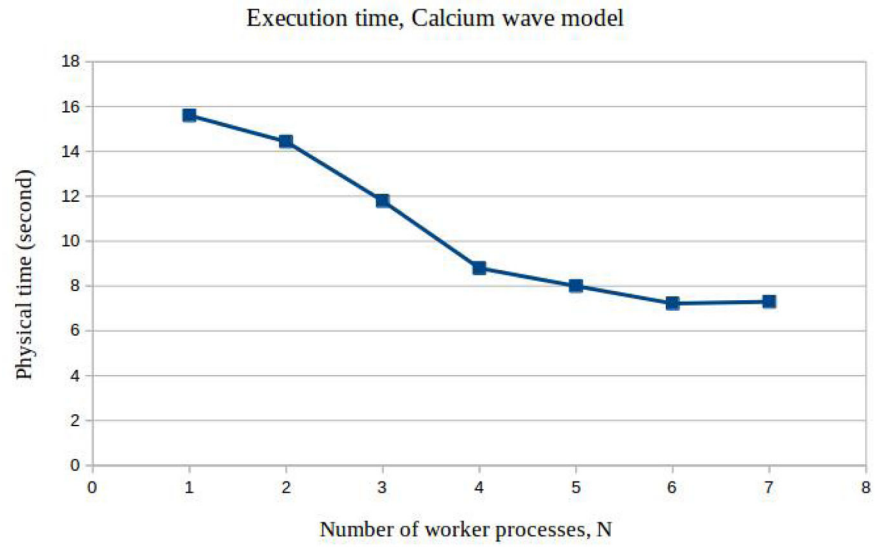


**Fig. 19.** Execution time of calcium wave model in parallel simulation.



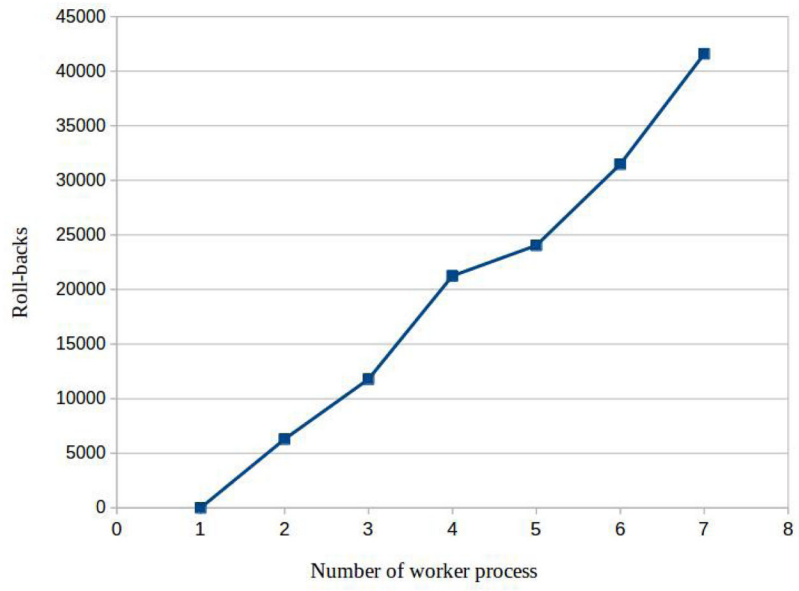


**Fig. 20.** Rollback with multiple worker processes in calcium wave model simulation.

**TABLE 1**

Performance table of calcium buffer model in parallel simulation

Number of workers, N	Average physical time, T(N), in sec.	Speedup, $S(N) = T(1)/T(N)$
1	2.53	1
2	1.27	1.993
3	0.96	2.66
4	0.68	3.7
5	0.57	4.44
6	0.48	5.27
7	0.46	5.5

Author Manuscript

Author Manuscript

Author Manuscript

Author Manuscript

**TABLE 2**

All constants for calcium wave model

$V_{IP_3R}$	0.0002
$K_{Act}$	0.0004
$K_{IP_3}$	0.0013
$K_{inh}$	0.0019
$K_{SERCA}$	0.0001
$V_{SERCA}$	.00003249
$V_{Leak}$	0.00003

Author Manuscript

Author Manuscript

Author Manuscript

Author Manuscript

**TABLE 3**

Experimental data of workloads of the covered and uncovered areas.

Description	Virtual Time = 4		Virtual Time = 8		Virtual Time = 12	
	Covered area	Uncovered area	Covered area	Uncovered area	Covered area	Uncovered area
Average number of processed events, NOE	5017.13	196.04	8668.65	380.4	12100.58	564.5
Percentage of event processing	96.10%	3.90%	95.62%	4.38%	95.34%	4.66%
Number of Sub-volumes	46	154	88	112	100	100